

The stability of the terrestrial planets with a more massive "Earth"

Áron Süli^{1*}, Rudolf Dvorak² and Florian Freistetter³

¹*Eötvös Loránd University, Department of Astronomy, Pázmány Péter sétány 1/A, Budapest, H-1518, Hungary*

²*University of Vienna, Institute of Astronomy, Türkenschanzstrasse 17, A-1180, Vienna, Austria*

³*Astrophysikalisches Institut und Universitäts-Sternwarte, Schillergäßchen 2-3, D-07745 Jena, Deutschland*

ABSTRACT

Although the long-term numerical integrations of planetary orbits indicate that our planetary system is dynamically stable at least ± 4 Gyr, the dynamics of our Solar System includes both chaotic and stable motions: the large planets exhibit remarkable stability on gigayear timescales, while the subsystem of the terrestrial planets is weekly chaotic with a maximum Lyapunov exponent reaching the value of $1/5 \text{ Myr}^{-1}$. In this paper the dynamics of the Sun–Venus–Earth–Mars–Jupiter–Saturn model is studied, where the mass of Earth was magnified via a mass factor κ_E . The resulting systems dominated by a massive Earth may serve also as models for exoplanetary systems that are similar to our one. This work is a continuation of our previous study, where the same model was used and the masses of the inner planets were uniformly magnified. That model was found to be substantially stable against the mass growth. Our simulations were undertaken for more than 100 different values of κ_E for a time of 20, in some cases for 100 Myrs. A major result was the appearance of an instability window at $\kappa_E \approx 5$, where Mars escaped. This new result has important implications for the theories of the planetary system formation process and mechanism. It is shown that with increasing κ_E the system splits into two, well separated subsystems: one consists of the inner, the other one consists of the outer planets. According to the results the model became more stable as κ_E increases and only when $\kappa_E \geq 540$ Mars escaped, on a Myr timescale. We found an interesting protection mechanism for Venus. These results give insights also to the stability of the habitable zone of exoplanetary systems, which harbour planets with relatively small eccentricities and inclinations.

Key words: celestial mechanics – Solar System: general.

1 INTRODUCTION

The determination of the stability of our Solar System is one of the oldest problems in astronomy. The question has been debated over more than 300 years, and has attracted the attention of many famous mathematicians over the course of history. The problem played a central role in the development of non-linear dynamics and chaos theory. Despite the considerable efforts, we do not possess a definite answer to the question of whether our Solar System is stable or not. This is partly a result of the fact that the definition of the term stability is not unambiguous when it is used in relation to the problem of planetary motion. In addition to the vagueness of the concept of stability, the planets in our planetary system show a character typical of dynamical chaos. The physical basis of this chaotic behaviour is now partly understood as a consequence of reso-

nance overlapping and three body resonances (Lecar et al. 2001; Murray & Holman 1999; Nesvorný & Morbidelli 1999) which can manifest themselves in dramatic and relatively sudden changes in an orbit. In the last two decades several numerical stability studies were performed in order to throw light on the question. At present the longest numerical integrations published are those of Ito & Tanikawa (2002), where six long-term numerical integrations of all nine planets, covering a time-span of several 10^9 and 10^{11} years are discussed. Their fundamental conclusion is that the Solar System seems to be stable in terms of the Hill-criteria at least over a time-span of ± 4 Gyr. Moreover it turned out that during the integration period all the planetary orbital elements have been confined in a narrow region.

On the other hand according to Laskar's semi-analytical secular perturbation theory (Laskar 1988), the terrestrial planets', especially Mercury's and Mars' eccentricities and inclinations show large and irregular variations on a timescale of several 10^9 year (Laskar 1996).

* E-mail: a.suli@astro.elte.hu (ÁS)

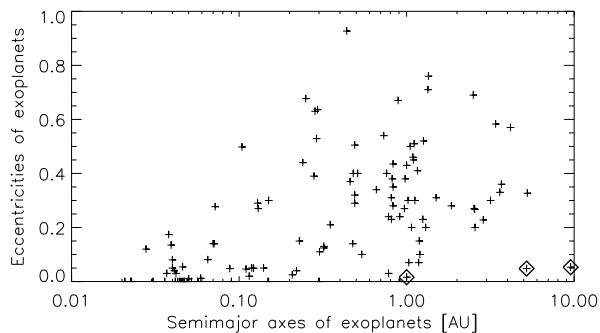


Figure 1. Eccentricities vs. the semimajor axes of the observed extrasolar planets. The x -axis is logarithmic. The positions of the Earth, Jupiter and Saturn are also indicated as diamonds with a plus sign in the middle.

Nowadays to study the stability of the Solar System, or its variants, as a representative of the different planetary systems has become part of the frontline research. Over the past few years the detection of planets outside the Solar System, the so called exoplanets, has greatly stimulated the stability studies of planetary systems. New exoplanets are being discovered on a regular basis; more than 150 (April, 2005) exoplanets are now known. There are 136 systems consisting of a central star and a gaseous giant planet, and 14 multiple systems with two, three and four planets. The so far discovered exoplanets have a minimum mass range ($m \cdot \sin(i_p)$) from $0.042 m_J$ to $17.5 m_J$ where m_J is Jupiter’s mass and i_p is the inclination of the orbital plane with respect to the plane of the sky. Since i_p is unknown a precise mass cannot be determined, only a lower mass limit. Because of the technical limitations only planets of Neptune mass or above can be detected and then only if they are less than 5 AU or so from the star ¹. Therefore more than 90 % of these planets are orbiting their host star well inside Jupiter’s orbit. There are major differences between the characteristics of the so far observed systems and those of the Solar System. Most of the planets have minimum masses substantially greater than that of Jupiter – up to six or even more times the mass of Jupiter. Dozens of planets are orbiting very close to their hosting star, with semimajor axes down to 0.04 AU. Finally, planetary orbits are found with large eccentricities, up to approximately 0.7, plus a few greater, significantly greater than the highest eccentricities observed for planets in our Solar System. These characteristics are depicted in Fig. 1, where the planets’ eccentricities are plotted against their semimajor axes, the locations of the Earth, Jupiter and Saturn are marked as diamonds. From Fig. 1 it is apparent that our planetary system may serve as model case for those planetary systems which have small eccentricities. Presumably these are also the ones where we may expect stable terrestrial planets moving in habitable zones (Asghari et al. 2004).

In previous papers (Dvorak & Süli 2002; Dvorak et al. 2005) the dynamical evolution of a simplified Solar system was studied. The model consisted of the Sun, the three most

massive terrestrial planets (Venus, Earth, Mars), Jupiter and Saturn. The masses of the inner planets were uniformly magnified by a mass factor κ . It turned out that the different systems remained stable up to 10 Myr for $\kappa \leq 220$. Stable islands were found for $\kappa = 245$ and 250, which is a well-known property in such regions which are close to the last stable orbit in the chaotic domain. We have shown that the dynamical coupling of Venus and Earth and that of Jupiter and Saturn remained unbroken for all studied κ . On the other hand the motion of Mars was not coupled to any other planet, what may be a reason for the fact that it was always Mars which caused the decay of the system after close approaches with Earth. However the remarkable stability of these model planetary systems suggests that exoplanetary systems with configuration like our Solar System may harbour moderately or even very massive terrestrial-like planets.

In the present work our aim was to study and analyze the dynamical evolution and the stability of the system with respect to the masses involved. Contrary to our previous study, in the present work only the mass of the Earth was increased via a mass factor κ_E . Furthermore, the examined systems may be considered as models for individual exoplanetary system, and the results can be applied to them. Section 2 explains our dynamical model, the applied methods and section 3 is devoted to a detailed description of the results in the $\kappa_E \in [1, 600]$ region. Finally, we discuss the results and the implication for exoplanetary systems.

2 DESCRIPTION OF THE MODEL AND METHODS

The applied dynamical model consisted of the Sun, Venus, Earth, Mars, Jupiter and Saturn. We have chosen this model for two reasons. To speed up the numerical integrations, we have omitted Mercury, Uranus and Neptune. Because of the small mass of Mercury, it only slightly perturbs the motion of the terrestrial planets and it has a short orbital period which would require a reduction in the integration step-size resulting in increased CPU time. Even though Uranus and Neptune are massive planets, they are evolving around the Sun more than twice as far as Saturn, and so they do not influence the motion of the inner planets significantly. These simplifications are also justified by the fact, that the dynamics of the inner planets are dominated by Jupiter and Saturn. Furthermore the so far observed exosystems harbour at most three of four planets. The above modification of the Solar System gives grounds for the adjective “simplified”. Hereafter we will refer to our simplified Solar System as S^3 . The other reason was to make the model more like an exoplanetary system. The mass of the Earth was magnified via a mass factor κ_E (the masses of the other planets were unaltered), which resulted in such hypothetical planetary systems, whose characteristics agree very well with several exosystems (for example if we multiply the semimajor axes of the planets of 47 Ursae Majoris by 2.5, the resulting configuration is something like the Sun, Jupiter and Saturn system, if $\kappa_E=1$). According to these modifications, our models are parallel with those exosystems, which harbour planets with small eccentricities and inclinations. In Fig. 2 the masses of the planets are plotted as a func-

¹ With OGLE, which is based on optical gravitational lensing it is possible to detect exoplanets with only Earth-mass.

tion of κ_E . At $\kappa_E \approx 90$ Earth is as massive as Saturn and when $\kappa_E \approx 300$ Earth is as massive as Jupiter. The mass of the other planets are plotted by horizontal dashed lines. The mass distribution of the so far discovered exoplanetary systems is also depicted in Fig. 2 up to mass parameter = 2. The integrations were done in the $\kappa_E \in [1, 600]$ region, which approximately corresponds to $0 < \text{mass parameter} \approx 2$ interval, and therefore the mass distribution in Fig. 2 is displayed only in this interval.

We have considered the S^3 as a non-linear Hamiltonian system, governed only by classical Newtonian gravitational forces between the objects of the model. The planets have been taken as point masses, and the Earth's Moon was not included in the models. The initial planetary orbital elements and the actual masses are listed in Table 1.

To check whether the different S^3 setups belonging to different κ_{ES} could be stable over a long time interval we utilized the very precise numerical integration scheme, the Lie-integrator method. This method is based on the integration of differential equations with Lie-series and uses the property of recurrence formulae for the Lie-terms. The details of the method are described in Hanslmeier & Dvorak (1984) and Lichtenegger (1984). The scheme is particularly effective in the case of highly eccentric orbits. The accuracy of this integration technique is based on an automatic stepsize control, and it has been checked in several comparative test computations with other integrators. Although symplectic integrators are very effective when eccentricities remain small, but the Lie-integrator is a better choice in studies, where very large eccentricity orbits may occur.

The length of the integrations was fixed at 20 Myrs, in some cases at 100 Myrs, which was a trade-off between too long CPU time and the quality of the results. Since our interest focuses primarily on the inner three planets' motions, for which the orbital time-scales are much shorter than those of the outer two giant planets, the 20 Myrs seems a justifiable choice, although it is known from earlier work (see for e.g. Jones et al. (2001); Jones & Sleep (2002)) that exosystems can stay stable for hundreds of millions of years and then fall apart. In the case of weak chaos therefore the 100 and especially the 20 Myr timespan might be short and in some of the integrations where the terrestrial planets survived for 20 or 100 Myrs, they might not survive significantly longer. For the sake of a comparison all results were derived on the same computer. In some cases we have performed comparative integrations on different platforms (to obtain more information of the particular system).

The conservative definition of the point at which systems become unstable is when close encounter between two planets happens: two bodies approach one another within an area of the larger Hill radius. The consequence of such an event is the dramatic changes in the orbital elements of the two planets, and usually the escape of the planet with smaller mass. In this paper we define a system unstable, when an orbit crossing or a close encounter happens. This definition is somewhat more general and the instability can be directly connected to the eccentricity via the perihelia and aphelia distances. Henceforward we state that our model is dynamically unstable if orbit crossing or close encounters happen in the course of the integration. Using both criteria is clearly an extension of the conservative definition of instability. It is justifiable to incorporate the orbital crossing

criteria in the definition since we know from experience that an orbital crossing in general leads to a close encounter in very short time. The main difference between the two definitions is the time-scale of instability. We note that orbital crossing does not lead to close encounter in all cases when certain resonances have adjusted the planetary motions in such a way that the planets avoid each other. For example this is the case in the Neptune-Pluto pair. In our models no such protection resonances are present, henceforward we use the above definition to distinguish between stable and unstable S^3 setups. The integrations were not stopped after one of the above criterion had been met, but were continued until the integration timespan was reached.

For an indication of stability we used a straightforward check based on the eccentricity. This osculating orbital element shows the probability of orbital crossing and close encounter of two planets, and therefore its value provides information on the stability of the orbit. We examined the behavior of the eccentricities of the planets along the integration, and used the largest value as a stability indicator; in the following we call it the maximum eccentricity method (hereafter MEM). This is a reliable indicator of chaos, because the overlap of two or more resonances induce chaos and large excursions in the eccentricity. We know from experience, that instability comes from a chaotic growth of the eccentricity. This simple check has already been used in other stability studies, and was found to be quite a powerful indicator of the stability character of an orbit (Dvorak et al. 2003; Asghari et al. 2004).

2.1 The Laplace-Lagrange secular theory

In order to find a theoretical explanation for the decay of the system we have applied the Laplace-Lagrange first order secular theory. This linear theory yields accurate results under the following assumptions:

- (i) no mean motion commensurabilities,
- (ii) no orbit-crossing, and
- (iii) the eccentricities and inclinations are small enough.

Our models meet these criteria. However a complication is that the orbits of Jupiter and Saturn are close to a 5:2 commensurability. Since the appearance of the Laplace-Lagrange theory, as a first approximation it has been extensively used in the studies of motion of the planets and of other Solar System bodies. In several researches (Knezević 1986; Laskar 1988) the results of the first and higher order secular theories were compared. According to these studies the secular frequencies calculated from the Laplace-Lagrange theory are sufficiently accurate for our present research goal. The main discrepancies are in the case of Jupiter and Saturn. As we are interested only in the motions of the inner planets, therefore we will apply the Laplace-Lagrange theory to our models. From the above assumptions it is apparent that the precision of the theory does not depend on the planetary masses, accordingly there is no theoretical limitation on the mass factor's magnitude.

Since the eccentricities and inclinations may vanish at remote epochs, it is better to use the Lagrange orbital elements:

$$\begin{pmatrix} h \\ k \end{pmatrix} = e \cdot \begin{pmatrix} \sin \varpi \\ \cos \varpi \end{pmatrix}, \quad \begin{pmatrix} p \\ q \end{pmatrix} = i \cdot \begin{pmatrix} \sin \Omega \\ \cos \Omega \end{pmatrix}. \quad (1)$$

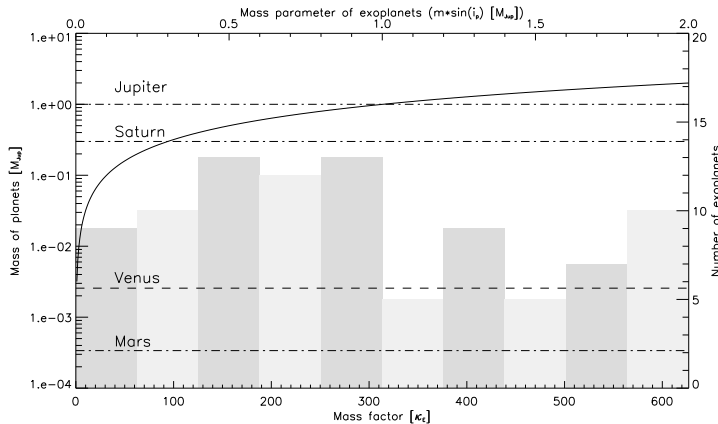


Figure 2. The mass distribution of the known exoplanetary systems are plotted together with the mass of the Earth as a function of the mass factor (κ_E) (solid line). The masses of the other planets were left unchanged, and they are represented by straight, dashed lines. The lower x -axis is the mass factor, the upper x -axis is the mass parameter of the exoplanetary system. The left y -axis is the mass of the planets in a logarithmic scale, the right y -axis is the number of planets. The width of the bin is 0.2 (this refers to the top axis)

Table 1. Planetary orbital elements (JD 2449200.5) with respect to the mean ecliptic and equinox J2000. The quantities a , e , i , ω , Ω and M denote the semimajor axis, eccentricity, inclination, argument of perihelion, longitude of ascending node and mean anomaly. In the last row the masses of the planets in Solar mass units are listed ($M_{Sun} = 1$).

	Venus	Earth	Mars	Jupiter	Saturn
a	0.723328	0.999999	1.523614	5.202627	9.545509
e	0.006747	0.016716	0.093443	0.048370	0.052420
i	3.394820	0.000545	1.850191	1.304638	2.485620
ω	54.847892	113.611521	286.492727	275.222227	338.025839
Ω	76.691772	349.288391	49.573832	100.470086	113.651098
M	135.521541	78.172620	185.208769	233.733076	259.852365
$1/m_i$	408 523.71	332 946.047	3 098 708.0	1047.348	3497.898

Eq. (1) associates the h , k , p and q Lagrangian-elements to the e , i , ϖ , and Ω Keplerian-elements, where e denote the eccentricity, i the inclination, ϖ the longitude of perihelion and Ω the longitude of ascending node. Using these variables the general solution of the differential equations for the planets takes the following form:

$$\begin{pmatrix} h_s \\ k_s \end{pmatrix} = \sum_{j=1}^n M_s^{(j)} \frac{\sin}{\cos} (g_j t + \beta_j), \quad (2)$$

$$\begin{pmatrix} p_s \\ q_s \end{pmatrix} = \sum_{j=1}^n L_s^{(j)} \frac{\sin}{\cos} (f_j t + \gamma_j), \quad (3)$$

where the s index denotes the planet, the j index denotes the mode, N is the number of planets, $M_s^{(j)}$ and $L_s^{(j)}$ are the amplitudes, g_j and f_j denote the secular frequencies and β_j and γ_j are the angular phases.

The planet's orbital elements are described by Eq. (2) and Eq. (3), which are the sum of harmonic oscillations. Using these formulae it can be calculated that the planet's eccentricities and inclinations are varying between given limits with quasiperiodic oscillations. Due to the positive g_j secular angular velocities the apsidal lines of the planets are rotating directly, whereas the nodes accordingly to the negative f_j

secular angular velocities are rotating indirectly. Upon these mean rotations quasiperiodic variations are superimposed. Both of the apsidal and nodal motions can be approximated by average angular velocities, which are to a first approximation equal with the frequencies of those harmonious terms which are multiplied by the largest amplitudes:

$$e_s \cdot \frac{\sin \varpi_s}{\cos \varpi_s} \approx M_s^{(J)} \frac{\sin}{\cos} (g_J t + \beta_J) \quad (4)$$

where $M_s^{(J)} = \max_j |M_s^{(j)}|$ and the average angular velocity of the s 'th planet is given by g_J .

In this manner on the basis of the amplitudes each secular frequency can be associate with each planet. This association is not mutually unambiguous. It may happen to associate a certain secular frequency to more then one planet.

The use of the linear theory seems to be in contradiction to the large eccentricities and inclinations that may be reached by a planet during the simulation. We emphasize that the forementioned theory was used at the beginning of the integration, when the inclinations and the eccentricities are small, and the above assumptions are therefore fulfilled.

The above described linear secular theory was implemented in the MAPLE computer algebra program. With

Table 2. Summary of the integrations.

κ_E interval	$\Delta\kappa_E$	Earth mass in Jupiter mass	Total time [Myr]
1 – 25	1.0	[1/300 – 1/12]	20
4 – 6	0.1	[1/75 – 1/50]	100
30 – 200	5.0	[1/10 – 2/3]	20
210 – 300	10.0	[2/3 – 1]	20
330 – 600	30.0	[1 – 2]	20

the aid of this application the formulae of the theory can be evaluated in a few seconds and it gives the complete first order solution of the problem.

3 RESULTS

In this section we give a detailed description and overview of the results of our simulations. The model was integrated for more than 100 different values of κ_E . The interval of data output was 100 years, the total amount of data is approximately 6 GBs, and the total used CPU time is more than several thousands of days. All of the integrations were done on two Sun Fire 15000 supercomputers with 72 US-III+ 1200 MHz processor in each computer. In Table 2 the first column lists the different κ_E intervals, the second shows the stepsize ($\Delta\kappa_E$) in the mass factor. A small stepsize is taken for $4 \leq \kappa_E \leq 6$ in order to explore the interesting behaviour of the system leading – very surprisingly – to the escape of Mars. In the third column we list approximately the mass of Earth in Jupiter’s mass unit. The last column gives the time-span of numerical integrations.

3.1 The $1 \leq \kappa_E \leq 25$ region

As we expected, the orbital motions of the planets indicate long-term stability in most of our numerical experiments: no orbital crossings nor close encounters between any pair of planets took place in the course of the integrations. However, a surprising result was the discovery of the instability window for the $\kappa_E \in [4, 6]$ interval: at several κ_E values Mars escaped; the details can be found in the next subsection.

Fig. 3 depicts the results of the MEM. The maximum eccentricities (hereafter ME) of Jupiter and Saturn are actually constant, with a value of 0.06, and 0.088, respectively (they are not shown in Fig. 3). As one can clearly see from Fig. 3 the MEs of the Earth and Venus are relatively small, and both curves show a similar behaviour as a consequence of the well-known coupling between them. We note, that the ME of Earth for $\kappa_E = 1$ is 60% greater than for $\kappa_E = 2$. After some oscillations of Venus’ and Earth’s MEs, they stay almost constant with a value of 0.041 and 0.035, respectively. In turn, the ME of Mars steadily increases with κ_E , and at $\kappa_E = 5$ it suddenly reaches a very high value, $e_{Mars} = 0.26091$ (the perihelion distance of Mars is $q_{Mars} = 1.126$)! After this peak Mars’ ME drops down to its starting value 0.1231, and begins to increase slowly and gradually with κ_E .

The character of the variation of the planetary orbital elements does not change substantially over the course of the simulation, except for κ_E around 5. The variations of

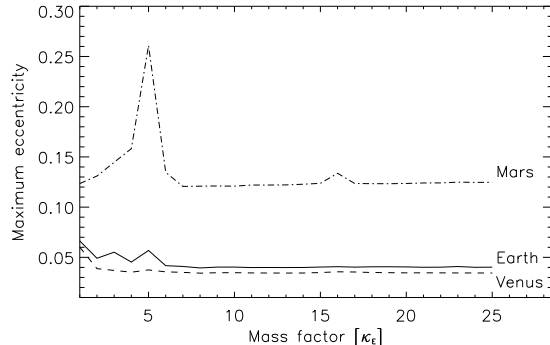


Figure 3. Results of the MEM in the $1 \leq \kappa_E \leq 25$ region ($\Delta\kappa_E = 1$). The x -axis is the κ_E , the y -axis is the maximum eccentricity (ME).

the semimajor axes are in the order of 10^{-4} – 10^{-3} AU for the inner planets, and for Jupiter and Saturn they are approximately 10^{-3} , 10^{-2} AU, respectively. The variations in Jupiter’s and Saturn’s semimajor axes are one order of magnitude larger than those of the inner planets, which is a consequence of the 5:2 near commensurability between their motion. For all simulations in this mass factor region the behaviour of the semimajor axes did not change, and their excursions remained in the above range.

The eccentricities as a function of time of the inner planets for $\kappa_E = 1, 2$, and 15 are shown in Fig. 4 (for the sake of a comparison the eccentricities for the actual masses are also depicted). As κ_E goes from 1 to 2, there is a substantial change in e for all three terrestrial planets. According to the MEM analysis (see Fig. 3), the MEs of Earth and Venus decrease, which manifests themselves in greater perihelia and smaller aphelia distances (see Fig. 4b). These changes decrease the probability of a close encounter between Venus and Earth, as can be inferred from Fig. 4b. Beyond this κ_E value the behaviour of Earth’s and Venus’ eccentricities do not change and in general their orbits turns into a more and more regular, quasiperiodic ones as κ_E increases. Moreover their dynamical coupling strengthens. These features can be traced on the panels of Fig. 4.

In the case of Mars the character of the variation of the eccentricity is more complex:

- For the actual masses Mars’ eccentricity fluctuates with an amplitude of 0.1 and with a very long period of approximately 2.5 Myrs. To this fluctuation smaller amplitudes with shorter periods are added. It is clear from Fig. 4a that Mars’ motion is not coupled to any of the other two terrestrial planets.
- At $\kappa_E = 2$ Mars’ eccentricity shows a quite different behaviour: it oscillates with a very short period around a mean eccentricity of 0.1 with an amplitude of about 0.02. With increasing κ_E the center of oscillation shifts to higher values, and reaches its maximum at 5, where the system is destabilized.
- For $\kappa_E > 5$ the motion of Mars gradually turns into a regular one. Moreover, dynamical coupling develops between all the three inner bodies, which is very well visible from Fig. 4c.

The terrestrial planets seem to gradually form a subsystem

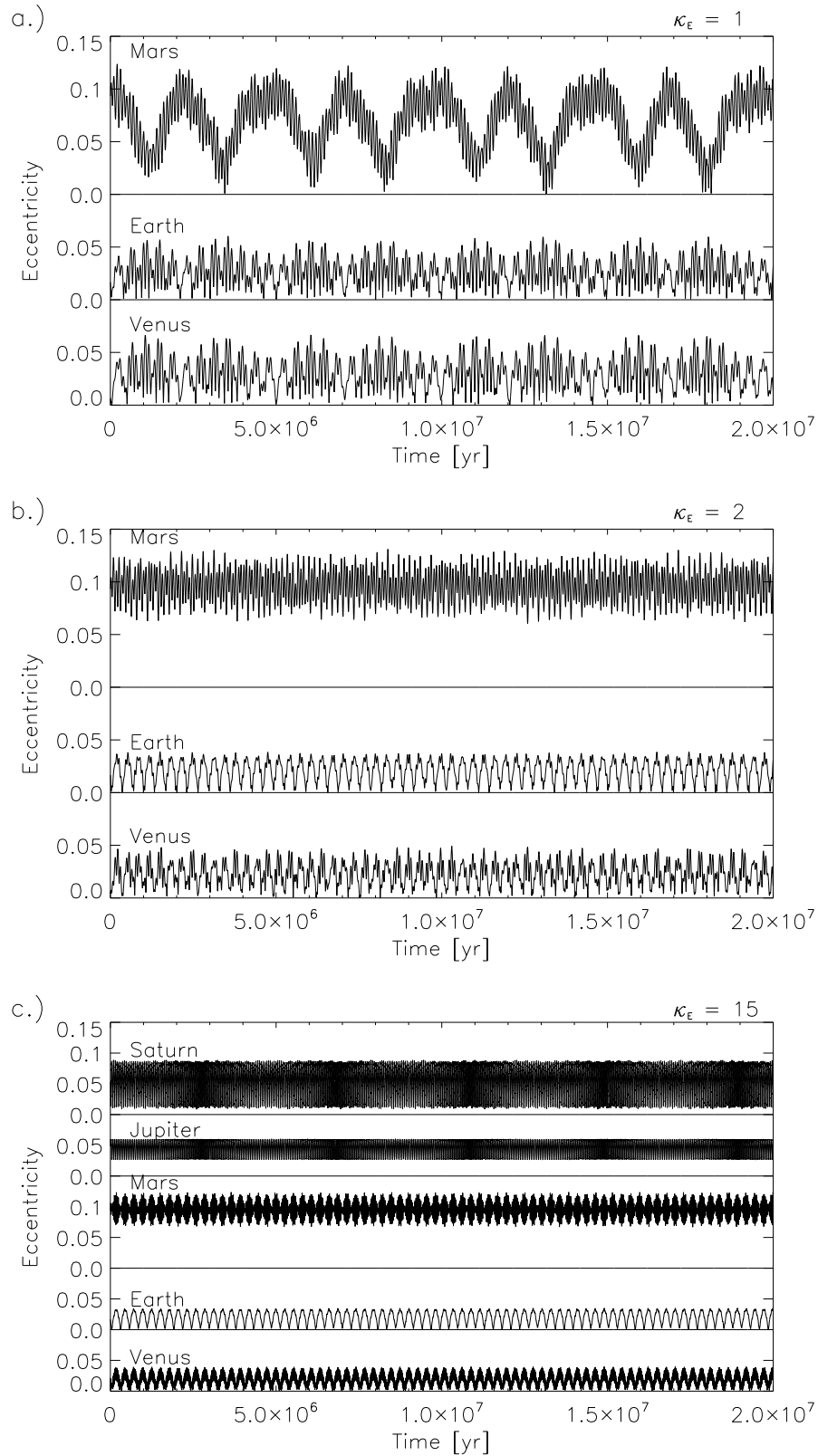


Figure 4. The eccentricities of the inner planets are shown as a function of time for the $\kappa_E = 1, 2, 15$ simulations. The time and mass factor evolution of the planets' eccentricities can be traced on the panels. On panel 4c. also Jupiter's and Saturn's eccentricities are shown: the existence of the two separate subsystems is well visible.

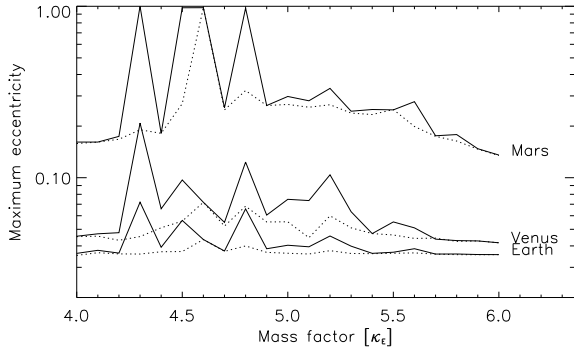


Figure 5. Results of the MEM in the $4 \leq \kappa_E \leq 6$ region. The dotted lines show the ME of the 20 Myr, whereas the solid lines show the ME of the 100 Myr integrations. The MEs of Jupiter and Saturn are not plotted. The instability window occupies the (4.2, 4.9) region. We note that the ordinate is logarithmic.

as the mass factor increases. As the Earth becomes the dominant planet in this region and the motions of the two smaller neighboring planets are influenced primarily by the Earth (the major variation in the eccentricities of the Earth, Venus and Mars has the same period, see Fig. 4c). With regard to this we may consider the inner planets as a collection of dynamically mutually dependent planets, namely a subsystem.

In this mass factor region the giant planets move on quiet orbits for the duration of all numerical integrations. Jupiter and Saturn also constitute a subsystem which is practically not affected from the terrestrial planets. An analysis of the eccentricities of all bodies for the subsequent mass factors shows that the model graduates into a system which consists of two separate and loosely dependent subsystems.

3.2 The instability window at $\kappa_E \approx 5$

According to Fig. 3 the ME of Mars reached its maximum value at $\kappa_E = 5$. To explore the dynamical evolution of the inner planets in more detail simulations were performed in the $\kappa_E = [4,6]$ region, with a stepsize of 0.1 for 100 Myrs. The results of the MEM are shown in Fig. 5, where several peaks ($e_M = 1.0$) in the curve of Mars' ME are visible, which correspond to escape orbits. We note that there are two minima: at 4.4 and at 4.7. This feature is typical of chaotic systems, where small differences in initial conditions, round off errors or the applied computing architectures may result in different outcomes. To verify this, the two systems with $\kappa_E = 4.4$ and 4.7 were integrated on different computers and both of the systems decayed. After $\kappa_E = 5.2$ the ME of Mars gradually drops down and at $\kappa_E = 6$ it is already less than 0.15.

Fig. 6 shows the evolution of the perihelia (q) and apelia (Q) distances of the inner planets for $\kappa_E = 4.6$, for which case we measured the shortest dynamical lifetime. A striking feature is that Mars' perihelion begins to decrease right at the start of the integration, as a consequence of the steep increase of its eccentricity. At 250 000 yr Mars' e reaches 0.16 then it decreases to 0.13, around this value it oscillates for 1 Myrs. Conversely, q and Q of the Earth and Venus stay in a well defined zone. At ~ 1.5 Myr, the perihelion of Mars begins to oscillate with quite a large amplitude. The center

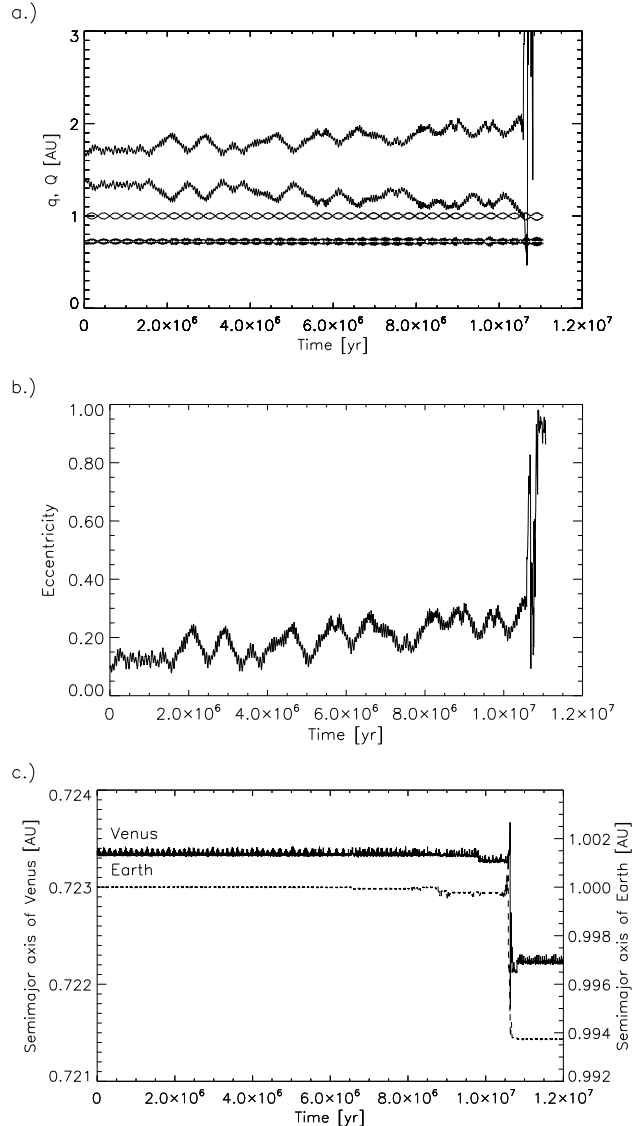


Figure 6. a.) the inner planets' perihelia (q) and apelia (Q) distances are shown as a function of time for the $\kappa_E = 4.6$ simulation. b.) The eccentricity of Mars is depicted. Note that Mars' orbit is excited to high eccentricity and it becomes Earth-crossing at $t \approx 10.5$ Myr. c.) The semimajor axes of the Earth and Venus are shown together.

of this oscillation grows secularly and after 10.5 Myr Mars becomes an Earth-crosser, moreover it crosses the orbit of Venus too. As a consequence of the several close encounters with Earth; Mars escapes from the system. This cascade mechanism is shown in Fig. 6c, where the semimajor axes of the Earth and Venus are plotted.

Because of the chaotic nature of the system, different dynamical lifetimes for the different κ_E values were found. Out of the 21 integrations for 100 Myr, Mars escaped four times and the system decayed². It must be stressed that the chosen length of the integration time is a problem, because

² By the decay of the system, we understand that the system has evolved into a different one, with a completely distinct configuration.

it may be relatively short for such investigations. It is well-known that there exist orbits which are stable for a very long time interval and then, all of a sudden they evolve into chaotic orbits. These 'sticky orbits' are common in nonlinear dynamical systems and therefore they exist also in planetary systems (Dvorak et al. 1998; Jones & Sleep 2002). This class of orbits are embedded in those region of the phase space, where regular and irregular orbits are close to each other. We suspect that those systems which did not decay, may be 'sticky systems', and will be unstable at a much longer time.

According to the chaos theory the extent of this instability window is a function of the numerical resolution (in our case the $\Delta\kappa_E$). Therefore it is not possible to find the exact size of this window, however with our resolution this instability window is in the interval $4.2 < \kappa_E < 4.9$

The surprising increase in the eccentricity of Mars may be a result of some secular resonances between the secular frequencies g_j and f_j . Such phenomena were already found by Laskar in the Solar System, who reported that large and irregular variations can appear in the eccentricities and inclinations of the terrestrial planets, especially of Mercury and Mars on time scales of several Gyr (Laskar 1996).

The secular variations of the orbital elements of the planets are calculated by means of the Laplace-Lagrange theory. Using our MAPLE application the $M_s^{(j)}$ and $L_s^{(j)}$ amplitudes, the g_j and f_j secular frequencies and β_j and γ_j were calculated in the $\kappa_E \in [4,6]$ interval on a very fine grid with a stepsize $\Delta\kappa_E = 0.001$. In this region two frequencies, f_2 and f_3 have almost the same value (see Table 3), while the other ones are well separated. In Table 3 the $f_5 = 0.0$ frequency is not included, and also the corresponding amplitude ($2.8402 \cdot 10^{-2}$) and the angular phase ($106^\circ.17$) were left out.

To visualize the dependence of f_2 and f_3 on the mass factor, they are shown in Fig. 7a, while in Fig. 7b their difference around $\kappa_E = 5$ is depicted. From Fig. 7b it is obvious, that the two curves do not intersect each other: the difference between the two frequencies are several orders of magnitudes greater than the accuracy of the computation, which was set to 10^{-10} . The $\Delta f = f_2 - f_3$ difference reaches its smallest value for $\kappa_E = 5.03$, $\Delta f = 0.1439$ "/yr, which is at the border of the aforementioned instability window.

A study of Table 3 shows that the largest amplitude are, in the solution for Mars, $L_3^{(2)}$ and $L_3^{(3)}$, for Jupiter $L_4^{(2)}$ and $L_4^{(3)}$ and for Saturn $L_5^{(2)}$, $L_5^{(3)}$. Accordingly the f_2 and f_3 frequencies, as was described in section 2.1, can be associated with Mars, Jupiter and Saturn. The orbital plane of Mars therefore rotates together with those of Jupiter and Saturn, giving rise to chaotic behaviour. The equality of two apsidal or nodal rates is referred to in Solar System as a secular resonance. In this case we have three secular resonances: $\dot{\Omega}_M \approx \dot{\Omega}_J$, $\dot{\Omega}_M \approx \dot{\Omega}_S$ and $\dot{\Omega}_J \approx \dot{\Omega}_S$. We suspect that these secular resonances are the possible source of the observed chaos, and produce the instability window.

3.3 The $30 \leq \kappa_E \leq 600$ region

Fig. 8 summarizes the results of the MEM in the $30 \leq \kappa_E \leq 600$ region. As one can clearly see from Fig. 8 the MEs of the planets gradually increase. None of the curves show any peaks, consequently in this region no instability window was

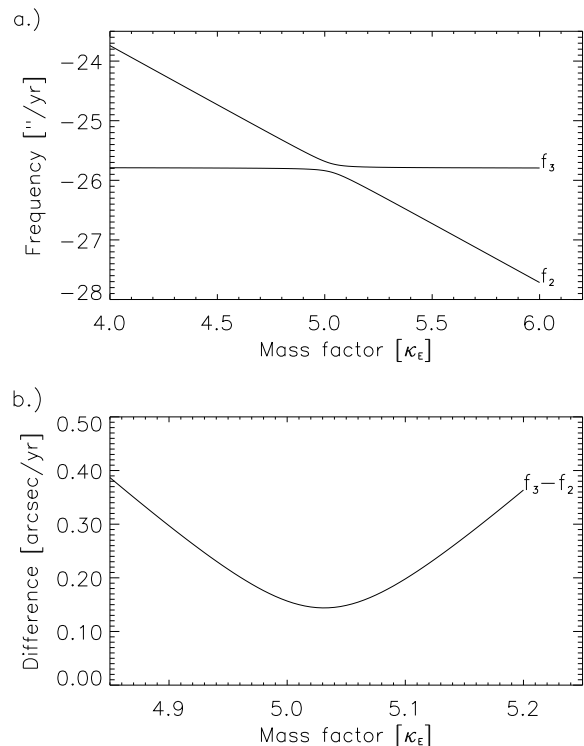


Figure 7. On the a.) panel are the f_2 and f_3 secular frequencies, on the b.) panel their difference around 5.0 are plotted versus the κ_E mass factor.

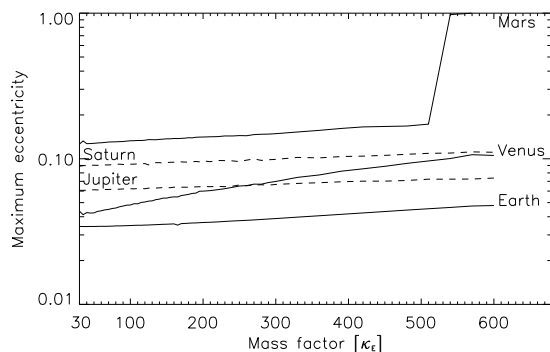


Figure 8. Results of the MEM in the $30 \leq \kappa_E \leq 600$ region. Note, that the y axis is logarithmic.

found. These numerical results are in line with the results of the linear theory. In this region each of the secular frequencies have quite different values. Beyond $\kappa_E \geq 540$ Mars escaped in all simulations. The MEs of the Earth, Jupiter and Saturn behave very similarly and we may say that from $\kappa_E = 100$ on the system is dominated by these planets and Venus and Mars may be considered as quasiasteroids.

Generally the semimajor axes of the inner planets are confined in a narrow stripe in the order of 10^{-4} – 10^{-3} AU. These stripes are defined by a very short quasiperiodic oscillation around the mean values of the planets' semimajor axes. As the mass factor increases the amplitudes of the oscillations grow, the width of these stripes slightly broadens.

Table 3. The f_j secular frequencies, the γ_j phases and the $L_s^{(j)}$ amplitudes of the model for $\kappa_E = 5.03$ calculated using the Lagrange-Laplace theory. The f_j are given in arcsec/yr and the γ_j s in degree.

f_j	-47.381072	-25.862186	-25.718241	-7.157383
γ_j	76°.92	306°.01	128°.89	297°.61
$L_s^{(j)}$				
Venus	5.2399 · 10 ⁻²	7.5778 · 10 ⁻³	1.0696 · 10 ⁻²	2.5795 · 10 ⁻²
Earth	-7.7184 · 10 ⁻³	3.9381 · 10 ⁻³	5.9598 · 10 ⁻³	2.3939 · 10 ⁻²
Mars	2.4032 · 10 ⁻³	-4.2737 · 10 ⁻¹	-4.3543 · 10 ⁻¹	1.3348 · 10 ⁻²
Jupiter	4.5852 · 10 ⁻⁶	3.1885 · 10 ⁻³	-3.1088 · 10 ⁻³	-1.2056 · 10 ⁻⁴
Saturn	-2.2595 · 10 ⁻⁶	-7.7642 · 10 ⁻³	7.7424 · 10 ⁻³	-1.8405 · 10 ⁻⁴

The typical evolution of the eccentricity of the inner planets are shown in Fig. 9. The character of the curves are similar to Fig. 4c, only the periods are shorter.

Since Venus, Earth and Mars have the same period in their eccentricities – just like the Jupiter and Saturn pair does – the system is separated into two subsystems: one consisting of Venus, Earth and Mars, and the other Jupiter and Saturn. This behaviour was already observed for smaller mass factor values. The strong coupling of the eccentricities of the two giant planets remains unbroken for all κ_E . The eccentricities of Venus and Mars are mainly determined by that of the Earth, which is the superposition of a long period ($T_l \sim 2.5 \cdot 10^5$ yr) variation with amplitude 0.035 and several shorter period ($\sim 10^4$ yr) and smaller amplitude variations (see Fig. 9b). In the case of Venus, upon this long period variation several very short periods are superimposed (see Fig. 9a). On the contrary the eccentricity of Mars flickers with a period T_l around 0.1 (see Fig. 9c).

As the mass factor increases the long period variations in the eccentricities of Jupiter and Saturn are more and more influenced by the Earth. In order to conserve the total angular momentum of the system the centers of oscillations of Jupiter's and Saturn's eccentricities are anticorrelated with the eccentricity of the Earth (see Fig. 10b). In spite of the large perturbations from the Earth, the coupling between the motion of Jupiter and Saturn are still very well determined (see Fig. 10a). This result is also supported by our previous study Dvorak & Süli (2002), and therefore we may say that the dynamical coupling of Jupiter and Saturn essentially determines the dynamics of the Solar System's bodies.

The time developments of the inclinations are very similar to those of the eccentricities:

- the variations of Jupiter's and Saturn's inclinations are coupled,
- the inclinations of Venus and Mars are primarily determined by that of the Earth,
- with growing κ_E Jupiter's and Saturn's inclinations are increasingly influenced by the Earth.

When $\kappa_E = 540$ Mars' eccentricity had grown secularly and at $T_e \approx 3.4$ Myr, Mars passed near by Earth, which ejected the planet from the system (see Fig. 11). In this case, we did not observe orbit-crossing. However the minimum distance between Earth and Mars was 0.164 AU, which is about twice the Hill radius of the massive "Earth" $R_H(\kappa_E = 540) = 0.081$ AU. A cataclysmic outcome is therefore to be expected (Jones et al. 2005). In the systems with $\kappa_E = 570$

and 600 Mars was ejected after a sequence of orbit-crossing with Earth at $T_e \approx 4.35 \times 10^6$ and at $T_e \approx 5.51 \times 10^6$ years, respectively.

The stability of Venus is an intriguing property of the systems. In each of our simulations the orbital elements of Venus did not show any sign of chaos. The Earth and Venus are prevented from close encounters by a coupling of Venus' eccentricity and $\Delta\varpi$; $\Delta\varpi$ is the difference between the longitude of perihelion of the Earth and Venus. Whenever the perihelion of Earth conjunctions with the aphelion of Venus ($\Delta\varpi = 180^\circ$), the eccentricity of Venus is around its minimum (see Fig. 12), maximizing the distance between the two orbits. A similar protection mechanism also occurs with real Mars and the asteroid Pallas. This kind of coupling was also observed by Jones & Sleep (2002) for an 'Earth' in the 47 UMa system.

4 DISCUSSION

We studied the dynamics of a simplified dynamical model of the Solar System where we included the three terrestrial planets Venus, Earth and Mars and the gas giants Jupiter and Saturn. This model was already studied in detail (Dvorak & Süli 2002) when the masses of all terrestrial planets were uniformly increased. It turned out that the different systems remained stable for 10 Myrs up to large mass factor values. As a continuation of this work the same model with a more massive Earth was studied and signs of chaotic behaviour were reported in Dvorak et al. (2005). In this article a detailed exploration of the different S^3 setups is presented, and the existence of an instability window is revealed. As an important byproduct the plethora of the integrations can serve as a general model of exoplanetary systems with two massive planets close to the 5:2 mean motion resonance on low eccentric orbits for comparable mass ratios of the giant planets.

We investigated over 100 S^3 models where we increased the mass of the Earth by a mass factor κ_E between $1 \leq \kappa_E \leq 600$. These new systems have been integrated using extensive numerical integrations for 20 million years (for selected systems up to 100 million years) to find out the effect of a very massive Earth on the stability of the whole system on one hand; on the other hand the model now can serve as example of exoplanetary systems of two or three massive planets.

It turned out, that even when the Earth had Jupiter's mass ($\kappa_E \approx 300$) and beyond, the system was still stable, but

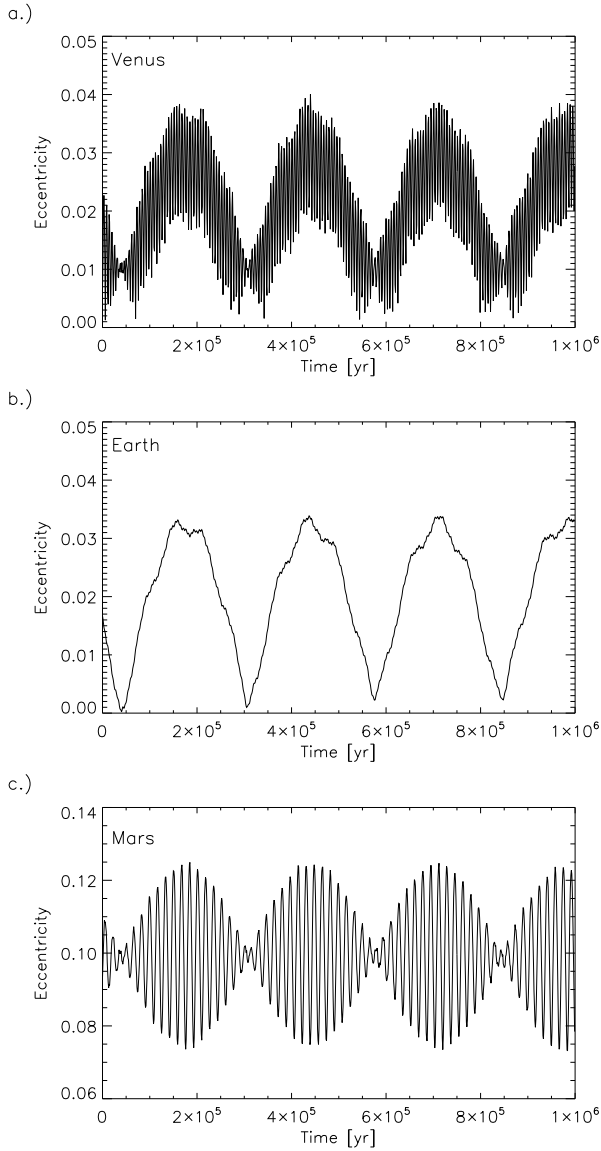


Figure 9. The eccentricities of the Venus, Earth and Mars (from top to bottom) for $\kappa_E = 30$ over a 1 million year time-span.

when $\kappa_E \in (4.2, 4.9)$, the motion of Mars become chaotic. In this instability window Mars' orbital eccentricity finally reached values which led to close encounters of Mars with the Earth, and even with Venus. After a sequence of close encounters Mars escaped within some millions of years. Using the results of the Laplace-Lagrange secular theory we found secular resonances acting between the motions of the nodes of Mars, Jupiter and Saturn. These secular resonances give rise to strong chaos, which is the cause of the appearance of the instability window, and eventually the escape of Mars.

We also found an interesting coupling of Venus' e and $\Delta\varpi$, which protect Venus from a close encounter with Earth. This mechanism was observed in the Solar System and in 47 UMa with a hypothetical Earth (Jones et al. 2005; Jones & Sleep 2002).

According to these results, the stability of the Solar System depends on the masses of the planets, and small changes in these parameters may result in a different dynamical evo-

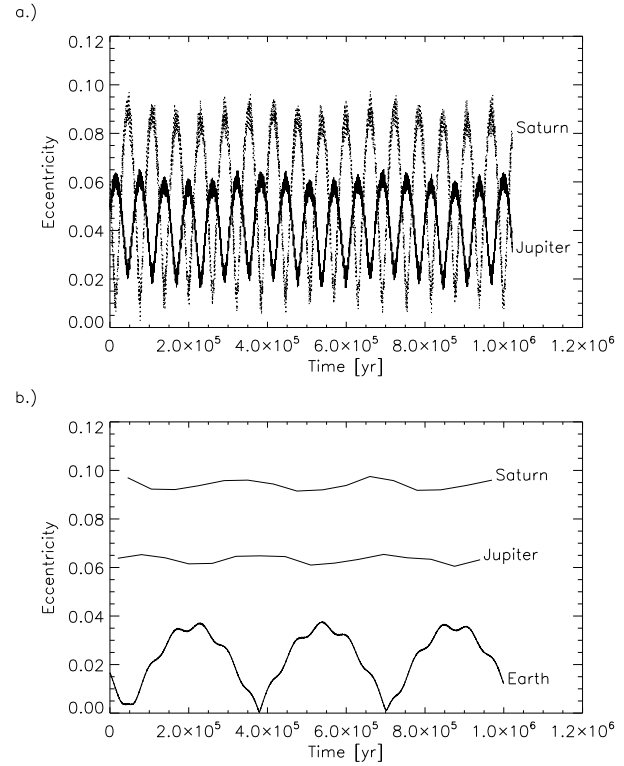


Figure 10. a.) The time development of the eccentricities of Jupiter and Saturn. b.) The eccentricity of the Earth and the local maximums of Jupiter's and Saturn's eccentricities are shown for $\kappa_E = 250$. The coupling between the eccentricities can be well observed.

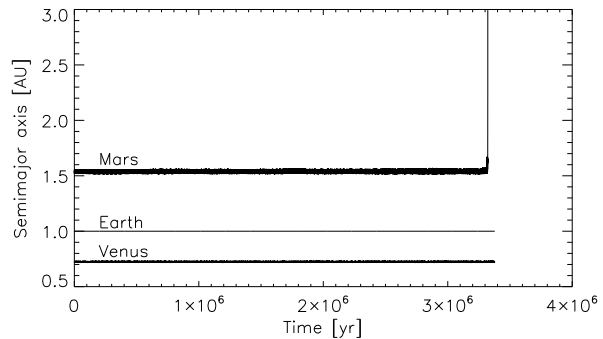


Figure 11. This plot shows the escape of Mars for $\kappa_E = 540$.

lution of the planetary system. No other instability window in κ_E were found; first results of additional computations where we increased the masses of Venus and separately also of Mars, showed signs of chaotic motions for some windows in κ too, but a detailed study of these two other cases of a modified S^3 is in preparation. There we also intend to give a detailed comparison of the three systems, namely with a massive Venus, a massive Earth and a massive Mars.

Finally we note that all these models may be used as dynamical reference models for a better understanding of the stability of orbits in extrasolar planetary systems.

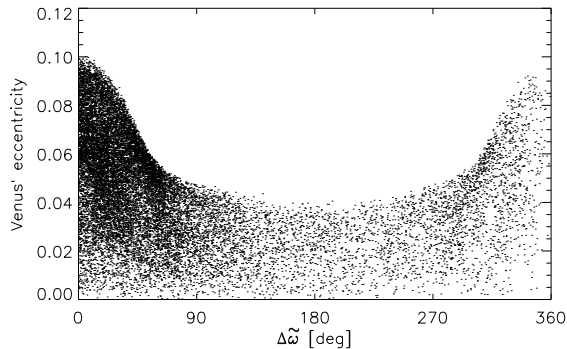


Figure 12. This plot shows the relationship between Venus' eccentricity and $\Delta\varpi$ during 20 Myrs for $\kappa_E = 540$.

ACKNOWLEDGMENTS

We would like to thank Professor B. Érdi for a critical reading of the original version of the paper and also the anonymous referee for several comments which greatly improved the clarity of the paper. We thank the Wissenschaftlich-Technisches Abkommen Österreich-Ungarn Projekt A12-2004, and the Hungarian Scientific Research Fund T043739. All numerical integrations were accomplished on the NI-IDP (National Information Infrastructure Development Program) supercomputer in Hungary.

References

- Asghari N. et al., 2004, *A&A*, 426, 353
 Dvorak R., Süli Á. and Freistetter F., 2005, in eds. Z. Knezević IAU Colloq. 197, Dynamics of populations of planetary systems, p. 63
 Dvorak R., Pilat-Lohinger E., Funk B., Freistetter F., 2003, *A&A*, 398, L1
 Dvorak R., Süli Á., 2002, *Celest. Mech. & Dyn. Astron.*, 83, 77
 Dvorak R., Contopoulos G., Efthymiopoulos Ch., Voglis N., 1998, *Planetary and Space Science*, 46, 1567
 Hanslmeier A., Dvorak R., 1984, *A&A*, 132, 203
 Ito T., Tanikawa K., 2002, *MNRAS*, 336, 483
 Jones B. W., Sleep P. N. Chambers J. E., 2001, *A&A*, 366, 254
 Jones B. W., Sleep P. N., 2002, *A&A*, 393, 1015
 Jones B. W., Underwood D. R., Sleep P. N., 2005, *ApJ*, 622, 1091
 Knezević Z., 1986, *Celest. Mech.*, 38, 123
 Laskar J., 1988, *A&A*, 198, 341
 Laskar J., 1996, *Celest. Mech. & Dyn. Astron.*, 64, 115
 Lecar M., Franklin F.A., Holman M.J., Murray N.W., 2001, *Annu. Rev. A & A*, 39, 581
 Lichtenegger H., 1984, *Celest. Mech.*, 34, 357
 Murray N., Holman M., 1999, *Sci.* 283, 1877
 Nesvorný D., Morbidelli A., 1999, *Celest. Mech. & Dyn. Astron.*, 71, 243